Theoretical investigation on molecular structure, vibrational spectra, HOMO-LUMO, NBO analysis and hyperpolarizability of 2-(Trifluoroacetyle)acetophenone

M. Karunanidhi[1], V. Balachandran[2,*], K. Anitha[3], M.Karnan[1] and G. Ilango[4]

[1]Department of Physics, Srimad Andavan Arts and Science College, Tiruchirappalli 620 005, India.
[2]Centre for Research, Department of Physics, A.A. Government Arts College, Musiri 621 211, India.
[3]Department of Physics, Bharathidasan University Constituent College Lalgudi, Tiruchirapalli-621 601, India.
[4]Department of Physics, MIET Engineering College, Tiruchirapalli-620 007, India.

ARTICLE INFO

ABSTRACT

In this work, the experimental and theoretical spectra of 2-(trifluoroacetyle)acetophenone (2TFAAP) are studied and FT-IR and FT-Raman spectra of title molecule have been recorded in the region 4000–400cm^{-1} and 3500–100cm^{-1}, respectively. The structural and spectroscopic data of the molecule in the ground state have been calculated by using Hartree-Fock and density functional theory method with the B3LYP/6-31G basis sets. The vibrational frequencies are calculated and scaled values are compared with the experimental FT-IR and FT-Raman spectra. The DFT (B3LYP/6-31G) calculations are more reliable than the *ab initio* HF/6-31G calculations for the vibrational study of (2TFAAP). The optimized geometric parameters (bond lengths and bond angles) are compared with experimental values of the molecule. Stability of the molecule was analyzed using NBO analysis. Thermal properties of the molecule have been calculated for various range of temperature and HOMO-LUHO energies also calculated, it shows that the charge transfer occurs within the molecule.

1.Introduction

The acetophenone and its derivatives are of great interest in biological activity and widely used as a parent compound to make drugs. Acetophenone is a raw material for the synthesis of some pharmaceuticals and present invention to simulate of insulin and used as a therapeutic agent [1–2]. The aromatic compounds naturally occur higher amount in plants, are used for governing the physiological functions. The vibrational analyses of this molecule would be helpful for understanding the various types of bonding and normal modes of vibration. Density functional theory (DFT) approaches, especially those using hybrid functional, have been evolved to a powerful and very reliable tool and routinely used for the determination of various molecular properties. B3LYP functional has been previously shown to provide an excellent compromise between accuracy and computational efficiency of vibrational spectra for large and medium size molecules [3–6]. It is well known that vibrational frequencies obtained by quantum chemical calculations are typically larger than their experimental counterparts, and thus, empirical scaling factors are usually used to better much the experimental vibrational frequencies [7]. These scaling factors depend both on the method and basis sets used in calculations and they are determined from the mean deviation between the calculated and experimental frequencies [8, 9]. By using the DFT (B3LYP) method, we have calculated the geometric parameters and the vibrational spectrum of 2-(trifluoroacetyle) acetophenone in the ground state and compared with the experimental vibrational frequencies. In addition NBO,

frontier molecular orbital and thermodynamic analysis is also carried out.

2. Experimental details

The sample (2TFAAP) was purchased from the Lancaster Chemical Company, (UK) which is of spectroscopic grade and hence used for recording the spectra as such without any further purification with a purity of greater than 97% and it was used as such without further purification. The Fourier transform infrared (FT-IR) spectrum of the sample was recorded at room temperature in the region 4000–400 cm^{-1} using BRUKER-IFS spectrophotometer equipped with composition of the pellet. The signals were collected for 100 scans with a scan interval of 1cm^{-1} and at optical resolution of 0.4 cm^{-1}. The Fourier Transform Raman (FT-Raman) BRUKER-FRA 106/IFS 100spectrometer were used for the Raman spectral measurements at room temperature. The spectrometer consisted of a quartz beam splitter and a high sensitive germanium diode detector cooled to the liquid nitrogen temperature. The sample was packed in a glass tube of about 5 mm diameter and excited in the 180- geometry with 1064 nm laser line at 75mW power from a diode pumped air cooled-cw Nd:YAG laser was (used as an excitation source) wavelength in the region4000–100 cm^{-1}. The signals were collected for 300 scans at the interval of 1 cm^{-1} and optical resolution of 0.1 cm$^{-1.}$.

3. Computational details

3.1 Computational methods

The molecular structure of the (2TFAAP) in ground state is computed by performing both ab initio-HF and DFT (B3LYP) with HF/6-31G and B3LYP/6-31G basis sets.

The optimized structural parameters are used in the vibrational frequency calculations in HF and DFT methods. The minimum energy of geometrical structure is obtained by using level 6-31G basis sets. The theoretical results have enabled us to make the detailed assignments of the experimental IR and Raman spectra of the title molecule. Calculations of structural parameters, atomic charges, vibrational frequencies, IR and Raman intensities of the title compound (Fig. 1) were carried out using Gaussian09 program package [10] by using DFT and HF approaches. Electron correlations were included using Becke3–Lee–Yang–Parr (B3LYP) procedure [11-13].Prior to compare the calculated vibrational frequencies with the experimental counterparts the former have been scaled by appropriate scaling factors [14-17]. Theoretical vibrational spectra of the title compound were interpreted by means of potential energy distribution (PED) with the version V7.0-G77 of the MOLVIB program written by Sundius [18].

3.2 NBO and thermodynamic analysis

The natural bonding orbital (NBO) calculation was performed using NBO 3.1 program and was carried out in the Gaussian09W package [10] at the DFT/B3LYP level. The hyperconjugative interaction energy was deducted from the NBO analysis for (2TFAAP) molecule, the dipole moment; linear polarizability and first hyperpolarizability were obtained from molecular polarizabilities based on theoretical calculations. The electronic properties such as HOMO and LUMO energies were determined by B3LYP method with same basis set approach. Moreover, the changes in the thermodynamic functions (heat capacity, entropy, enthalpy and Gibb's free energy) were investigated for the different temperatures from the vibrational frequency calculations of title molecule.

4. Results and discussion

4.1. Molecular geometry

The optimized molecular structure of 2(trifluoroacetyle) acetophenone with atom numbering is shown in Fig. 1. By allowing the relaxation of all parameters, the calculations converge to optimize geometries, which correspond to true energy minima, as revealed by the lack of imaginary frequencies in the vibrational mode calculation. The most optimized bond lengths and bond angles of this compound are calculated by both HF and DFT (B3LYP) methods are listed in Table 1. The aromatic C–C bond distances of 2(trifluoroacetyle) acetophenone are found to have higher values in case of B3LYP calculation with respect to HF computation.
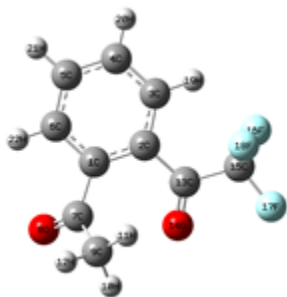
Fig 1. Optimized molecular structure of 2-(Trifluoroacetyle)acetophenone.

4.2. Vibrational analysis

The 60 normal modes of vibrations of 2-(trifluoroacetyle) acetophenone are distributed by symmetry species as vib = 3N – 6 =41A' (in-plane) + 19A" (out-plane)

It is in agreement with Cs point group symmetry. Here A' represents symmetric planer and A" asymmetric non-planer vibrations. The detailed vibrational assignment of the experimental wavenumbers is based on normal mode analyses and a comparison with theoretically scaled wavenumbers with PED by HF and B3LYP methods. Since the scaled wave numbers following B3LYP method are found closest to experimental data than the results obtained using other methods, so only the PEDs from this set of data are discussed in detail. The calculated frequencies are usually higher than the corresponding experimental quantities, due to the combination of electron correlation effects and basis set deficiencies. After applying the overall uniform scaling factor theoretical calculations reproduce the experimental data well in agreement. The observed FT-IR and FT-Raman spectra of 2-(trifluoroacetyle) acetophenone are shown in Figs. 2 and 3, respectively. The observed and scaled theoretical frequencies using DFT methods B3LYP/ 6-31G and HF/6-31G basis sets, IR intensities, and Raman activity of B3LYP/6-31G basis with PEDs are listed in Table 2.
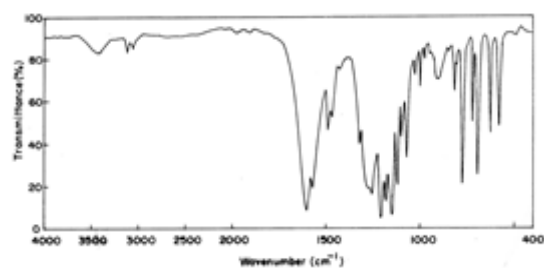
Fig 2. Observed FTIR spectrum of 2-(Trifluoroacetyle)acetophenone.
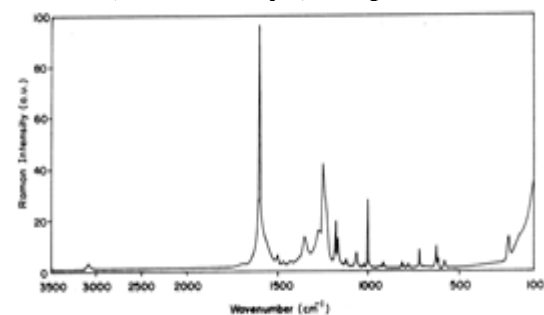
Fig 3. Observed FT-Raman spectrum of 2-(Trifluoroacetyle)acetophenone.

4.3. C–H vibrations

The acetyl substituted 2(trifluoroacetyle) acetophenone like molecules gives rise to C–H stretching, C–H in-plane and C–H out-of-plane bending vibrations. Aromatic compounds commonly exhibit multiple weak bands in the region 3100–3000cm^{-1} [19] due to aromatic C–H stretching vibrations. In the present study the C–H vibrations of the title compound are observed at 3104, 3026cm^{-1} in FTIR spectrum and the same type of vibrations are observed at 3098cm^{-1} in FT-Raman. All bands are medium intensity and in the expected region, but two vibrations are missing in the region due to overtone combinations. The theoretical wavenumbers due to C–H aromatic stretching are lie within the range 3105, 3096, 3025 and 3013cm^{-1} by B3LYP/6-31G and agreement with the results of Sundraganesan and coworkers [20]. In this region the bands are not appreciably affected by the nature of the substituent. The bands due to C–H in-plane bending vibration interact with C–C stretching vibrations, are observed as number of bands in the region 1465–1281cm^{-1} [21].

Table 1. Optimized structural parameters of 2(trifluoroacetyle)acetophenone utilizing HF/6-31G and B3LYP/6-31G density functional calculation.

Bond length	Value(A)		Bond angle	Value(A°)		Dihedral angle	Value(A°)	
	HF/6-31G	B3LYP/6-31G		HF/6-31G	B3LYP/6-31G		HF/6-31G	B3LYP/6-31G
C1-C2	1.405	1.422	C2-C1-C6	119.042	118.925	C6-C1-C2-C3	1.884	118.925
C1-C6	1.387	1.401	C2-C1-C7	125.162	125.234	C6-C1-C2-C13	-174.169	125.234
C1-C7	1.506	1.511	C6-C1-C7	115.791	115.834	C7-C1-C2-C3	-177.345	115.834
C2-C3	1.395	1.411	C1-C2-C3	119.443	119.340	C7-C1-C2-C13	6.601	119.340
C2-C13	1.473	1.471	C1-C2-C13	119.335	119.416	C2-C1-C6-C5	-1.881	119.416
C3-C4	1.384	1.395	C3-C2-C13	121.102	121.051	C2-C1-C6-H22	178.107	121.051
C3-H19	1.069	1.082	C2-C3-C4	120.772	120.757	C7-C1-C6-C5	177.419	120.757
C4-C5	1.384	1.398	C2-C3-H19	120.615	120.147	C7-C1-C6-H22	-2.592	120.147
C4-H20	1.072	1.084	C4-C3-H19	118.600	119.062	C2-C1-C7-O8	-127.442	119.062
C5-C6	1.387	1.399	C3-C4-C5	119.715	119.837	C2-C1-C7-C9	60.500	119.837
C5-H21	1.072	1.085	C3-C4-H20	119.764	119.746	C6-C1-C7-O8	53.306	119.746
C6-H22	1.071	1.084	C5-C4-H20	120.517	120.409	C6-C1-C7-C9	-118.752	120.409
C7-O8	1.218	1.243	C4-C5-C6	120.041	119.987	C1-C2-C3-C4	-0.652	119.987
C7-C9	1.505	1.515	C4-C5-H21	120.232	120.217	C1-C2-C3-H19	-179.301	120.217
C9-H10	1.080	1.093	C6-C5-H21	119.727	119.795	C13-C2-C3-C4	175.330	119.795
C9-H11	1.079	1.091	C1-C6-C5	120.957	121.094	C13-C2-C3-H19	-3.319	121.094
C9-H12	1.084	1.097	C1-C6-H22	118.892	118.432	C1-C2-C13-O14	13.807	118.432
C9-O14	2.889	2.858	C5-C6-H22	120.151	120.471	C1-C2-C13-C15	-166.514	120.471
H10-O14	2.781	2.730	C1-C7-O8	118.996	118.852	C3-C2-C13-O14	-162.179	118.852
H11-O14	2.774	2.727	C1-C7-C9	119.832	119.904	C3-C2-C13-C15	17.500	119.904
C13-O14	1.211	1.240	O8-C7-C9	120.686	120.703	C2-C3-C4-C5	-0.625	120.703
C13-C15	1.528	1.542	C7-C9-H10	109.622	109.761	C2-C3-C4-H20	-179.839	109.761
C15-F16	1.365	1.396	C7-C9-H11	113.219	113.393	H19-C3-C4-C5	178.050	113.393
C15-F17	1.347	1.371	C7-C9-H12	108.051	107.930	H19-C3-C4-H20	-1.163	107.930
C15-F18	1.364	1.393	C7-C9-O14	69.016	71.399	C3-C4-C5-C6	0.653	71.399
F18-H19	2.543	2.565	H10-C9-H11	109.263	109.219	C3-C4-C5-H21	-179.109	109.219

Table 2. Experimental and Calculated HF-B3LYP/6-31G levels of vibrational frequencies (cm^{-1}), IR intensity (kmmol^{-1}) and Raman activity (Å^4 amu^{-1}) of 2(trifluoroacetyle)acetophenone.

S.No	Spe.	Observed frequencies (cm^{-1})		Calculated frequencies (cm^{-1})				IR Intensity (kmmol^{-1})		Raman Activity (Å^4 amu^{-1})		Vibrational assignments /PED (≥ 10%)
				HF/6-31G		B3LYP/6-31G						
		IR	Raman	Unscaled	Scaled	Unscaled	Scaled	HF/6-31G	B3LYP/6-31G	HF/6-31G	B3LYP/6-31G	
1	A'	3104v		3428	3114	3261	3105	1.732	2.441	103.595	103.553	ν CH(90)
2	A'		3098v	3404	3102	3237	3096	8.757	9.776	131.215	149.838	ν CH(95)
3	A'	3026v		3392	3029	3226	3025	8.483	7.699	92.645	103.441	ν CH(98)
4	A'			3375	3018	3211	3013	2.287	2.351	60.606	64.633	ν CH(90)
5	A'			3328	3009	3178	3005	10.741	10.974	45.824	39.838	ν CH$_3$(90)
6	A'			3294	3002	3142	2997	10.358	7.144	62.417	67.374	ν CH$_3$(95)
7	A'			3215	2973	3064	2968	5.415	3.499	116.966	136.551	ν CH$_3$ (91)
8	A'	1602s		1914	1609	1696	1603	176.489	80.299	85.277	33.800	νCO(71), νCC(19), β CH(12)

9	A'		1592vs	1890	1593	1690	1590	186.539	160.253	23.718	67.448	$\nu CO(71)$, $\nu CC(19)$, β CH(12)
10	A'	1577v		1803	1578	1649	1575	13.772	33.837	65.400	85.369	$\nu CC(69)$, β CH(20)
11	A'		1503v	1764	1508	1617	1504	43.378	42.596	37.543	35.843	$\nu CC(71)$, β CH(17)
12	A'			1674	1492	1539	1489	9.823	11.731	9.519	8.985	ν CC(95)
13	A'	1468s	1470v	1639	1476	1522	1472	10.904	9.547	14.422	17.345	β CH$_3$(95)
14	A'	1436v		1631	1438	1516	1433	11.015	8.660	17.681	17.844	β CH$_3$ (97)
15	A'	1373v		1625	1375	1501	1371	5.776	3.119	1.563	0.807	β CH(70), ν CH$_3$ (10), $\nu CC(20)$
16	A'		1352m	1572	1359	1443	1351	24.413	27.194	4.758	7.666	β CH$_3$ (95)
17	A'		1319s	1480	1327	1370	1320	17.051	24.889	9.652	5.123	$\nu CC(90)$, β CH(10)
18	A'	1295v		1463	1303	1352	1296	34.534	5.501	1.257	0.426	β CH(70), (85), $\nu CC(15)$
19	A'	1231s	1232s	1392	1240	1337	1230	75.888	16.738	13.354	3.655	$\nu CC(60)$, β CH (30), γ CH(10)
20	A'	1192s		1384	1197	1282	1191	125.286	120.836	4.571	17.213	νCC (80), β CH(11)
21	A'	1169m	1171s	1363	1178	1237	1173	199.531	9.975	10.094	11.282	β CH(81), $\nu CF(18)$
22	A'		1158v	1315	1166	1223	1157	147.709	262.040	20.334	18.924	νCF_3 (80)
23	A'	1128s		1306	1135	1190	1129	235.592	87.930	5.482	2.757	$\nu CC(77)$, β CH(19)
24	A'		1118v	1299	1127	1163	1120	28.751	64.274	12.416	5.243	β CH (70), β CH$_3$ (20)
25	A'	1103s		1257	1113	1133	1106	47.364	211.438	5.102	1.752	$\nu CF_3(62)$, β CH(20), $\nu CC(13)$
26	A'	1077s		1213	1083	1115	1077	14.634	8.281	2.435	1.832	νCC (78), $\nu CH(14)$
27	A"	1060s	1063m	1201	1071	1085	1062	1.962	9.723	0.598	28.139	γ CH$_3$(70), $\nu CC(13)$
28	A"			1186	1047	1068	1040	6.107	1.717	3.758	8.805	γ CH$_3$ (75), $\nu CC(9)$
29	A'	1013m		1164	1020	1045	1013	1.092	2.899	23.609	0.083	νCC (82), γ CF(11)
30	A'	1000s	1000s	1145	1009	1015	1001	0.595	21.404	5.161	3.902	νCC (80), $\nu CC(14)$
31	A"	974m		1104	981	1001	970	27.400	3.535	4.835	0.581	γ CH (65)
32	A'	923v	920v	1050	930	977	921	13.890	103.752	2.356	2.081	β Ring
33	A"	887s		1040	891	928	885	124.446	5.146	2.081	3.781	γ CH(95)
34	A"	808m	808v	923	817	889	806	8.297	6.733	1.195	1.422	γ CH(68)
35	A"	769vs	766v	890	783	795	770	50.179	33.139	1.509	1.703	γ CH(78), γ CH$_3$(13)
36	A'		718m	829	727	765	718	4.943	6.386	0.601	0.739	β Ring
37	A"	706s		808	714	731	710	28.679	19.713	1.159	1.491	γ CF$_3$ (66), γ CC(32)
38	A"	682vs		772	690	708	682	6.817	1.556	16.139	16.535	γ CF$_3$ (85)
39	A'	628vs	628m	728	631	687	626	50.660	38.396	1.836	1.461	$\nu CF_3(70)$, Rtrigd(25)
40	A'			695	617	635	609	3.826	2.010	2.965	2.030	γ CC(62), ω CH$_3$ (34)
41	A'	588vs		660	593	605	588	27.786	14.852	1.653	4.427	βCO (61), $\nu CC(19)$, ω CH$_3$(18)
42	A'		583w	653	586	602	581	20.219	17.431	7.204	6.035	βCO (85), γ CH$_3$(11)
43	A"			593	530	539	521	9.094	5.858	1.565	1.066	γ CO (65), β CH$_3$(26)
44	A"	483v		551	495	500	482	16.366	8.627	2.412	2.816	γRing (57), δCF_3(35)
45	A"			522	462	475	453	3.234	1.670	3.54	4.210	β CF$_3$(51), β CH$_3$(45)
46	A"			484	419	436	409	1.345	1.028	1.389	1.451	γ CO (73), ρCF_3(21)
47	A"			444	403	404	391	7.864	5.140	0.874	0.637	γRing(73), δCF_3(21), γ CH(11)
48	A'			406	376	376	360	8.342	6.170	2.065	1.987	β CC (40) , γ CH(35) , β CH$_3$(14)
49	A'			370	333	342	321	0.788	0.804	2.854	2.766	β CC (45) , β CH$_3$(15), β CF(17)
50	A'			335	311	309	290	3.149	1.513	1.562	1.794	β CC (72), γCF_3(27)
51	A'			300	278	273	267	7.428	5.867	1.113	0.678	β CF$_3$ (55), CC(35) , γ CH3(14)
52	A"			267	217	239	203	4.801	3.015	0.924	0.831	γ CF$_3$ (68), tCF$_3$(32), γ CH$_3$(11)
53	A"		177m	197	189	190	175	7.309	5.880	0.967	0.748	γ CC (70), $\gamma CO(18)$

54	A"			194	173	179	162	1.396	1.994	1.594	1.932	γ CC (95) ,γCO (35),
55	A"			153	142	141	131	0.401	0.416	2.384	2.736	γ CC (65), γRing(28)
56	A'			120	119	108	102	0.149	0.293	2.05	1.811	tCH$_3$(95)
57	A'			116	109	103	97	1.697	1.068	3.694	3.961	ω CF$_3$(80)
58	A"			77	75	68	62	3.663	2.374	3.288	3.390	γ CC (72), γ CO (14)
59	A'			60	49	51	43	0.745	0.707	0.247	0.370	tCF$_3$(72), β CH$_3$(21)
60	A'			19	18	19	16	2.793	2.579	0.406	0.525	ω CH$_3$ (70), γ CO (14)

ν-stretching,β-in-plane bending, γ-out-of-plane bending, δ-scissoring, ω-wagging,ρ-rocking, twisting, Rtrigd-Ring trigonal deformation, βRing-in-plane ring,   γRing-out-of -plane ring.

Table 3. Accumulation of natural charges and electron population of atoms in core, valance, Rydberg orbitals of 2(trifluoroacetyl)acetophenone.

Atoms[a]	Charge (e)	Natural population (e)			Total (e)	Atoms[b]	Charge (e)	Natural population (e)			Total (e)
		Core	Valence	Rydberg				Core	Valence	Rydberg	
C7	0.5398	1.9992	3.4290	0.0320	5.4602	C1	-0.0594	1.9988	4.0462	0.0144	6.0594
H10	0.2851	0.0000	0.7138	0.0011	0.7149	C2	-0.1443	1.9989	4.1325	0.0130	6.1443
H11	0.2445	0.0000	0.7544	0.0012	0.7555	C3	-0.1875	1.9990	4.1774	0.0110	6.1875
H12	0.2691	0.0000	0.7297	0.0012	0.7309	C4	-0.2321	1.9990	4.2213	0.0118	6.2321
C13	0.4215	1.9990	3.5486	0.0308	5.5785	C5	-0.1962	1.9990	4.1859	0.0112	6.1962
C15	0.9992	1.9992	2.9527	0.0490	5.0008	C6	-0.2075	1.9990	4.1968	0.0117	6.2075
H19	0.2631	0.0000	0.7343	0.0026	0.7369	O8	-0.5156	1.9998	6.5117	0.0041	8.5156
H20	0.2571	0.0000	0.7420	0.0009	0.7429	C9	-0.7788	1.9992	4.7736	0.0060	6.7788
H21	0.2566	0.0000	0.7425	0.0010	0.7435	O14	-0.4658	1.9998	6.4609	0.0052	8.4658
H22	0.2681	0.0000	0.7302	0.0016	0.7319	F16	-0.3463	1.9999	7.3442	0.0021	9.3463
C7	0.5398	1.9992	3.4290	0.0320	5.4602	F17	-0.3244	1.9999	7.3223	0.0022	9.3244
H10	0.2851	0.0000	0.7138	0.0011	0.7149	F18	-0.3462	1.9999	7.3442	0.0021	9.3462

[a] Atoms containing positive charges
[b] Atoms containing negative charges

In this compound above vibrations are observed at 1295 and 1169cm^{-1} in FT-IR and 1171, 1118cm^{-1} in FT-Raman. The theoretically scaled vibrations by B3LYP/6-31G level method 1371, 1296, 1173 and1120 cm^{-1} are shows good agreement with experimentally recorded data. The C–H out-of-plane bending vibrations are appeared within the region 900–667cm^{-1} [22]. The vibrations identified at 1013, 974, 887, and 808,769cm^{-1} in FT-IR and 808,766cm^{-1} in FT-Raman are assigned to C–H in-plane bending. The calculated C–H out-of-plane bending vibrations by DFT method 1013, 970, 885, 806 and 770 cm^{-1} are also lie within the characteristic region.

4.5. C-C vibrations

Generally the C- C stretching vibrations in aromatic compounds are seen in the region of 1430–1650cm^{-1}. According to Socrates [22], For aromatic six-membered rings, e.g., benzenes and pyridines, there are two or three bands in this region due to skeletal vibrations, the strongest usually being at about 1500 cm^{-1}. For substituted benzenes with identical atoms or groups on all Para-pairs of ring carbon atoms, the vibrations causing the band at 1625 – 1590 cm^{-1} are infrared-inactive due to symmetry considerations, the compound having a center of symmetry at the ring center. If there is no center of symmetry and the vibrations are infrared-active [22]. As predicted in the earlier references, the prominent peaks at 1503 and 1577cm^{-1} are due to strong C–C stretching and 1319, 1232, 1231, 1192, 1128, 1118 cm^{-1} are due to strong C–C skeletal vibrations for 2TFAAP. These peaks are confirmed that the compound is aromatic in nature [23]. The peaks are assigned at 1063, 1060, 1000, 923, 920, 718 and 682cm^{-1} due to C–C–C in-plane bending vibrations and the peaks at 605, 602, 588, 583 and 483cm^{-1} are due to C–C–C out of plane bending vibrations. Except C–C stretching vibrations, all assignments are coherent with the literature data [24] and also the theoretically computed C–C–C vibrations by B3LYP/6-31G basis set shows good agreement with recorded spectral data. The C–C vibrations are pulled slightly to the lower region and are purely due to the slight-breakdown of hexagonal ring by the substitutions.

4.4. Methyl group vibrations

The methyl substituted C–H stretching vibrations usually appears below the range of aromatic C–H stretching.Methyl group vibrations are generally referred to as electron donating substituent in the aromatic rings system, the asymmetric C-H stretching mode of CH$_3$ is expected around 2980 cm^{-1} and the CH$_3$ asymmetric stretching is expected at 2870 cm^{-1} [25,26].The theoretically calculated values by B3LYP/6-31G method at 3005, 2992 and 2968 cm^{-1} are coherent with the literature data. The asymmetric and symmetric deformation vibrations of methyl group appear within the region 1465–1440cm^{-1} and 1390–1370cm^{-1} [25]. In the present investigation, the bands at 1468, 1436cm^{-1} in infrared with medium intensity 1470, 1433and 1352 cm^{-1} in Raman with strong intensity are observed as CH$_3$ asymmetric deformation and symmetric deformation vibrations. The theoretically calculated values by B3LYP/6-31G method at 1472, 1433 and 1351 cm^{-1} shows good agreement with experimental values. The methyl rocking mode vibration usually appears within the region 1070–1010cm^{-1} [26]. With reference to literature data, a band observed at 1041, 1063cm^{-1} in Raman spectrum and 1060cm^{-1} in FT-IR are assigned CH$_3$ rocking vibration. The DFT calculation gives rocking vibration at 1040 and1062cm^{-1} are quiet fit with experimental values. Torsional modes of vibrations are observed at very low frequencies. In this DFT study a frequency at 102cm^{-1} is assigned to torsional mode of vibration.

4.6. C=O vibrations

The characteristic infrared absorption frequency of C=O in acids are normally strong in intensity and found in the region 1800–1690cm^{-1} [27]. This position of C=O stretching more effective to analyze the various factors in ring aromatic compounds. The C=O bond formed by = bond between C and O intermolecular hydrogen bonding, reduces the frequencies of the C=O stretching absorption to a greater degree than does intermolecular H bonding because of the different electro-negativities of C and O, the bonding are not equally distributed between the two atoms. The loan pair of electrons on oxygen also determines the nature of the carbonyl groups. The C=O stretching bands of acids are considerably more intense than ketonic C=O stretching bands. In the present study the characteristic ketonic C=O frequency appears at 1602 cm^{-1} in FT-IR and, 1592 cm^{-1} in FT-Raman spectrum are assigned to C=O stretching vibration. The calculated values of 1609, 1593 and 1603, 1590 cm^{-1} at HF/6-31G and B3LYP/6-31G levels of theory are in good agreement with the experimental value of C=O stretching mode. This C=O vibration appears in the expected range shows that it is not much affected by other vibrations. Moreover, Kolev[28] showed that in aromatic and aliphatic ketones, the C=O in-plane and out-of-plane deformation modes are seen in 605–552 cm^{-1} and 584–285 cm^{-1} region, respectively. In our case C=O in-plane bending vibration for 2TFAAP is observed FT-IR band at 588 cm^{-1} and the FT-Raman band at 583 cm^{-1}. The theoretically calculated values by B3LYP/6-31G method at 581 and 588 cm^{-1} shows good agreement with experimental values and also the theoretically calculated values of C=O out-of-plane bending vibration by DFT method at 521 and 409 cm^{-1} are coherent with the literature data.

4.7. CF$_3$ vibrations

Aromatic fluorine compounds give stretching bands in the region 1270–1100 cm^{-1} [29]. Very strong bands at 1103 cm^{-1} in FT-IR spectrum and a medium band at 1158 cm^{-1} in FT-Raman spectrum for 2TFAAP are assigned to CF$_3$ stretching vibrations. The computation vibrations are assigned at 1157 and 1106 cm^{-1} by B3LYP/6-31G basis set reproduces the observed wave numbers. CF$_3$ in-plane bending vibration is expected in the range 420–254 cm^{-1}[30, 31]. The C-F in-plane bending modes are identified as very weak bands at 483 in FT-IR spectrum and DFT method gives the same mode at 482,453 cm^{-1}. The CF$_3$ out-of-plane bending vibrations are observed in the range 520–101 cm^{-1} [31, 32]. In 2TFAAP, weak FT-IR bands at 706 and 682 cm^{-1} are assigned to CF$_3$ out-of-plane vibration. These vibrations are assigned at 710 and 682 cm^{-1}by B3LYP/6-31G method are good agreement with experimental values. The CF$_3$ torsional modes of vibrations are observed at very low frequencies. In our theoretical study a frequency at 43cm^{-1} is assigned to CF$_3$ torsional mode of vibration.

5. Natural bond orbital (NBO) analysis

Natural bond orbital (NBO) analysis is a useful tool for understanding delocalization of electron density from occupied Lewis-type (donor) NBOs to properly unoccupied non-Lewis type (acceptor) NBOs within the molecule. The accumulation of natural charges on individual atom of the title molecule is given in Table 3. The stabilization of orbital interaction is proportional to the energy difference between interacting orbital. Therefore, the interaction having strongest stabilization takes place between effective donors and effective acceptors. This bonding,anti bonding interaction can be quantitatively described in terms of the NBO approach that is expressed by means of second-order perturbation interaction

energy E(2) [33–36]. This energy represents the estimate of the off-diagonal NBO Fock matrix element. The stabilization energy $E^{(2)}$ associated with i (donor)→ j (acceptor) delocalization is estimated from the second-order perturbation approach as given below $E^{(2)} = q_i \, F^{(2)} \, (I,j)/\varepsilon_j - \varepsilon_i$, where q_i is the donor orbital occupancy, ε_i and ε_j are diagonal elements (orbital energies) and F(i, j) is the off-diagonal Fock matrix element. The different types of donor–acceptor interactions and their stabilization energy are determined by second order perturbation analysis of Fock matrix of 2TFAAP. The stabilization energy of all lone pair–bond pair interactions and only bond pair–bond pair interactions are listed in Table 4. In 2TFAAP molecule, the lone pair donor orbital, $n_O \rightarrow \pi^*_{cc}$ interaction between the (O8) lone pair and the C7 antibonding orbital gives a strong stabilization of 19.180 kcal mol^{-1}. The n to the antibonding orbital (π^*) of (C13) is 15.880 kcal mol^{-1}. The bond pair donor → π^* stabilization energy of lone pair of electrons present in the oxygen atom (O14) orbital, $\pi_O \rightarrow \pi^*_C$ interactions give more stabilization than $\pi_F \rightarrow \pi^*_c$ and $\sigma_{cc} \rightarrow$

σ^*_{cc} interactions. The analysis of the natural bond orbital of 2TFAAP by B3LYP/6-31G method is carried out to provide the occupancy, contribution to the parent NBO and mainly on the percentage contributions of the atoms present in the bond. NBO analysis of molecules illustrate the deciphering of the molecular wave function in terms Lewis structures, charge, bond order, bond type, hybridization, resonance, donor–acceptor interactions, charge transfer and resonance possibility. Table 5 depicts the bonding concepts such as type of bond orbital, their occupancies, the natural atomic hybrids of which the NBO is composed, giving the percentage of the 29.14%NBO on each hybrid, the atom label and a hybrid label showing the hybrid orbital (spx) composition (the amount of s-character, p-character, etc.) of 2-(trifluoroacetyl) acetophenone determined by B3LYP/6-31G method. The occupancies of NBOs are reflecting their exquisite dependence on the chemical environment. The Lewis structure that is closest to the optimized structure is determined.

Table 4. Significant second-order interaction energy (E (2), kcal/mol) between donor and acceptor orbitals of 2(trifluoroacetyl)acetophenone calculated at B3LYP/6-31G level of theory.

r (i)	Acceptor (j)	E(2)[a] kcal/mol	$(\varepsilon_i - \varepsilon_j)$[b] a.u	F_{ij}[c] a.u	r (i)	Acceptor (j)	E(2)[a] kcal/mol	$(\varepsilon_i - \varepsilon_j)$[b] a.u	F_{ij}[c] a.u
σ(C1-C2)	σ*(C1-C6)	4.820	1.750	0.082	σ(C4-C5)	σ*(C5-C6)	3.430	1.760	0.070
σ(C1-C2)	σ*(C2-C3)	5.770	1.730	0.089	σ(C4-H20)	σ*(C5-C6)	4.310	1.540	0.073
σ(C1-C2)	σ*(C2-C13)	3.560	1.610	0.068	σ(C5-C6)	σ*(C1-C6)	4.120	1.750	0.076
σ(C1-C6)	σ*(C1-C2)	5.830	1.730	0.090	σ(C5-C6)	σ*(C1-C7)	3.350	1.590	0.066
σ(C1-C6)	σ*(C2-C13)	4.080	1.610	0.073	σ(C5-C6)	σ*(C4-C5)	3.410	1.760	0.069
σ(C1-C6)	σ*(C5-C6)	3.510	1.760	0.070	σ(C5-H21)	σ*(C1-C6)	4.780	1.540	0.077
σ(C1-C7)	σ*(C1-C2)	3.410	1.660	0.067	σ(C5-H21)	σ*(C3-C4)	4.490	1.550	0.074
σ(C1-C7)	σ*(C1-C6)	3.170	1.690	0.065	σ(C6-H22)	σ*(C1-C2)	5.650	1.500	0.082
σ(C1-C7)	σ*(C5-C6)	3.170	1.700	0.066	σ(C6-H22)	σ*(C4-C5)	4.360	1.530	0.073
σ(C2-C3)	σ*(C1-C2)	6.750	1.730	0.097	σ(C9-H10)	σ*(C7-O8)	5.520	0.880	0.063
σ(C2-C3)	σ*(C1-C7)	3.870	1.590	0.071	σ(C9-H11)	σ*(C7-O8)	5.270	1.480	0.079
σ(C2-C3)	σ*(C3-C4)	3.770	1.770	0.073	σ(C9-H12)	σ*(C7-O8)	7.340	0.880	0.073
σ(C2-C13)	σ*(C1-C2)	3.390	1.740	0.069	π(O8)	π*(C7)	19.180	1.820	0.167
σ(C2-C13)	σ*(C2-C3)	3.530	1.740	0.070	π(O14)	π*(C13)	15.880	1.890	0.155
σ(C3-C4)	σ*(C2)	3.270	2.260	0.077	π(O14)	π*(C2-C13)	3.550	1.670	0.069
σ(C3-C4)	σ*(C2-C3)	4.530	1.740	0.079	π(F16)	π*(C15)	7.020	2.330	0.114
σ(C3-C4)	σ*(C2-C13)	4.140	1.620	0.074	π(F16)	π*(C15)	3.930	2.280	0.084
σ(C3-C4)	σ*(C4-C5)	3.470	1.770	0.070	π(F17)	π*(C15)	7.630	2.420	0.121
σ(C3-H19)	σ*(C1-C2)	5.490	1.520	0.082	π(F17)	π*(C15)	4.880	2.250	0.094
σ(C3-H19)	σ*(C4-C5)	4.430	1.550	0.074	π(F18)	π*(C15)	4.740	2.440	0.096
σ(C4-C5)	σ*(C3-C4)	3.510	1.770	0.070	π(F18)	π*(C15)	5.920	2.330	0.105

[a] E(2) means energy of hyper[a] conjugative interactions.
[b] Energy difference between donor and acceptor i and j NBO orbitals.
[c] F(i,j) is the Fock matrix element between i and j NBO orbitals.

Table 5. Natural atomic orbital occupancies and energies of most interacting NBO's of 2(trifluoroacetyl)acetophenone along with their hybrid atomic orbitals and hybrid directionality.

Parameters[a] (A−B)	Occupancies	Energies (a.u)	Hybrid	AO(%)[b]
σ(C1-C2)	1.967	0.700	$sp^{1.87}(C_1) \, sp^{1.90}(C2)$	s(34.81)+p(65.19) s(34.46)+p(65.54)
σ(C1-C6)	1.969	0.716	$sp^{1.91}(C_1) \, sp^{1.9}(C6)$	s(34.33)+p(65.67) s(34.48)+p(65.52)
σ(C1-C7)	1.979	0.726	$sp^{2.24}(C_1) \, sp^{1.94}(C7)$	s(30.86)+p(69.194 s(34.06)+p(65.94)
σ(C2-C3)	1.972	0.718	$sp^{1.85}(C2) \, sp^{1.93}(C3)$	s(35.05)+p(64.95) s(34.08)+p(65.92)
σ(C2-C13)	1.979	0.714	$sp^{2.28}(C2) \, sp^{1.53}(C13)$	s(30.49)+p(69.51) s(39.58)+p(60.42)
σ(C3-C4)	1.979	0.713	$sp^{1.81}(C3) \, sp^{1.87}(C4)$	s(35.57)+p(64.43) s(34.81)+p(65.19)
σ(C3-H19)	1.979	0.796	$sp^{2.30}(C3) \, sp(H19)$	s(30.34)+p(69.66) s(100)
σ(C4-C5)	1.981	0.707	$sp^{2.87}(C4) \, sp^{1.86}(C5)$	s(34.84)+p(65.16) s(34.95)+p(65.05)
σ(C4-H20)	1.982	0.793	$sp^{2.29}(C4) \, sp(H20)$	s(35.35)+p(69.65) s(100)
σ(C5-C6)	1.979	0.706	$sp^{1.86}(C5) \, sp^{1.84}(C6)$	s(34.93)+p(65.07) s(35.15)+p(64.85)
σ(C5-H21)	1.982	0.793	$sp^{2.32}(C5) \, sp(H21)$	s(30.11)+p(69.89) s(100)
σ(C6-H22)	1.98	0.797	$sp^{2.29}(C6) \, sp(H22)$	s(30.37)+p(69.63) s(100)
σ(C7-O8)	1.995	0.587	$sp^{2.52}(C7) \, sp^{1.63}(O8)$	s(28.39)+p(71.61) s(37.99)+p(62.01)
σ(C7-C9)	1.988	0.705	$sp^{1.78}(C7) \, sp^{2.75}(C9)$	s(36.01)+p(63.99) s(26.69)+p(73.31)
σ(C9-H10)	1.973	0.800	$sp^{3.10}(C9) \, sp(H10)$	s(24.42)+p(75.58) s(100)
σ(C9-H11)	1.989	0.789	$sp^{2.96}(C9) \, sp(H11)$	s(25.24)+p(74.76) s(100)
σ(C9-H12)	1.968	0.794	$sp^{3.25}(C9) \, sp(H12)$	s(23.63)+p(76.37) s(100)
σ(C13-O14)	1.994	0.593	$sp^{2.30}(C_{13}) \, p^{1.63}(O14)$	s(30.33)+p(69.67) s(38.02)+p(61.92)
σ(C13-C15)	1.987	0.701	$sp^{2.36}(C_{13}) \, p^{1.84}(C15)$	s(29.80)+p(70.20) s(35.19)+p(64.81)
σ(C15-F16)	1.991	0.525	$sp^{3.71}(C15) \, p^{3.56}(F16)$	s(21.23)+p(78.77) s(22.92)+p(77.08)
σ(C15-F17)	1.993	0.528	$sp^{3.52}(C15) sp^{3.09}(F17)$	s(22.15)+p(77.85) s(24.44)+p(75.56)
σ(C15-F18)	1.991	0.525	$sp^{3.69}(C15) \, p^{3.50}(F18)$	s(21.33)+p(78.67) s(23.23)+p(76.76)

[a] For numbering of atoms refer Fig. 1
[b] Percentage of s-type and p-type subshell of an atomic orbitals are given in their respective brackets

For example, the bonding orbital for C1-C2 with 1.967 electrons has 50.58% C1 character in a $sp^{1.87}$ hybrid and has 49.42% C2 character in a $sp^{1.90}$ hybrid orbital. In the case of C7-O8 bonding orbital with 1.995 electrons has 34.49% C7 character and has 65.51% O8 character. A bonding orbital for C13-O14 with 1.994 electrons has 35.17% C13 character in a $sp^{2.30}$ hybrid and has 64.83% O14 character in a $sp^{1.63}$ orbital. The C15-F16 with 1.991 electrons has 27.56% C15 character in a $sp^{3.71}$ hybrid and has 72.44% F16 character in a $sp^{3.36}$ orbital. The C-C bonds of the aromatic ring posses more p character than s character. This is clearly indicates the delocalization of p electrons among all the carbon atoms. Similarly C13-O14 bond has also posses more p character. For the title compound the dipole moment; linear polarizability and first hyperpolarizability were obtained from molecular polarizabilities based on theoretical calculations are listed in Table 6.

Table 7. Mulliken population analysis of 2(trifluroacetyl) acetophenone performed at HF/6-31G and B3LYP/6-31G.

Atoms	Atomic charges	
	HF/6-31G	B3LYP/6-31G
C1	-0.0375	-0.0655
C2	-0.2740	-0.2879
C3	0.0218	0.0235
C4	-0.1121	-0.0754
C5	0.1235	0.0924
C6	-0.1804	-0.1217
C7	0.9053	0.8308
O8	-0.7819	-0.6384
C9	-0.0752	-0.1327
H10	0.0488	0.0516
H11	0.0067	0.0104
H12	0.0226	0.0266
C13	0.8781	0.7514
O14	-0.7298	-0.6103
C15	1.6016	1.4321
F16	-0.5664	-0.5122
F17	-0.5495	-0.4904
F18	-0.5628	-0.5042
H19	0.0868	0.0787
H20	0.0522	0.0399
H21	0.0501	0.0381
H22	0.0720	0.0635

6. Frontier molecular orbital's

Highest Occupied Molecular Orbital (HOMO) and Lowest Unoccupied Molecular Orbital (LUMO) are very important parameters for quantum chemistry. The energies of HOMO, LUMO and their orbital energies are calculated using B3LYP/6-31G method and the pictorial illustration of the frontier molecular orbitals are shown in Fig. 4. Molecular orbitals provide insight into the nature of reactivity and some of the structural and physical properties of molecules. The positive and negative phase is represented in red and green colour, respectively. The plots reveal that the region of HOMO spread over the entire molecule of 2TFAAP while in the case of LUMO it is spread over the entire molecule except on acetyl group. The calculated energy gap of HOMO–LUMO's explains the ultimate charge transfer interface within the molecule. The frontier orbital energy gap calculated by B3LYP/6-31G method (LUMO- HOMO) in case of 2TFAAP is found to be is -0.14483 a.u.
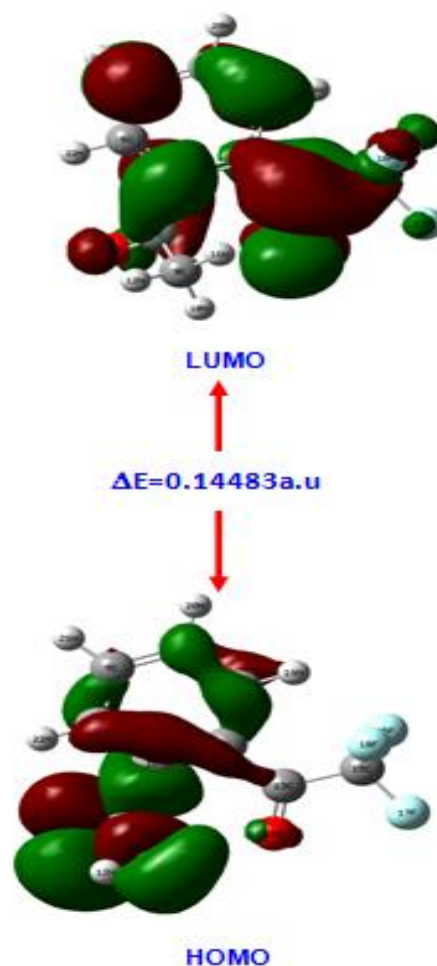
Fig. 4 HOMO-LUMO plot of 2-(Trifluoroacetyle)acetophenone.

7. Mullikan atomic charges

Mullikan [36] atomic charge calculation has an important role for the application of QCC of the molecular system. Atomic charge affects dipole moment, polarizability, electronic structure and other molecular properties of the system. The calculated Mullikan charge (e) values of 2TFAAP are listed in Table 7. It is clearly shown that the carbon atom attached with hydrogen atom is negative whereas the remaining carbon atoms are positively charged in the title compound.

The oxygen atoms have more negative charge whereas all the hydrogen atoms have the positive charges. The more positive charge of carbon is found for the compound C3, C5, C7 and C13; it is mainly due to the substitution of negative charge of fluorine and oxygen atoms. The lone pair of fluorine atoms (F16, F17 and F18) shows the charge transferred from C to F. Illustration of atomic charge plotted for HF/6-31G and B3LYP/6-31G levels have been shown in Fig. 5.
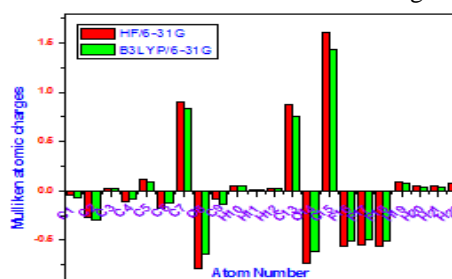
Fig. 5 Mulliken atomic charges of 2-(Trifluoroacetyle)acetophenone.

Table 6. The *Ab initio* HF/6-31G and B3LYP6-31G calculated electric dipole moments (Debye), Dipole moments compound, polarizability (in a.u), β components and β_{tot} (10^{-30} esu) value of 2(trifluoroacetyl)acetophenone.

Parameters	HF/6-31G	B3LYP/6-31G	Parameters	HF/6-31G	B3LYP/6-31G
μ_x	-1.2799	-1.1406	β_{xxx}	34.1957	40.2786
μ_y	4.2552	3.8664	β_{yyy}	26.4351	21.6038
μ_z	2.9045	2.4368	β_{zzz}	-1.6810	-2.4446
μ	5.3086	4.7104	β_{xyy}	7.8299	8.2984
α_{xx}	-92.7143	-90.4021	β_{xxy}	32.3022	29.0836
α_{yy}	-81.6810	-79.2286	β_{xxz}	21.0705	17.6243
α_{zz}	-89.7653	-86.8125	β_{xzz}	21.9653	20.2503
α_{xy}	-6.8816	-6.5747	β_{yzz}	-8.9339	-8.2664
α_{xz}	-7.2389	-5.9321	β_{YYZ}	15.4592	12.9494
α_{yz}	-6.6347	-5.5930			
$\Delta\alpha$(esu)	42.6718×10^{-25}	52.92251×10^{-25}	βtot(esu)	6.59×10^{-30}	6.39×10^{-30}

8. Thermodynamic properties

For the title compound, the standard thermodynamic functions: heat capacity ($C^0_{p;m}$), entropy (S^0_m) and enthalpy (H^0_m), Gibb's free energy (G^0_m) were calculated based on the vibrational analysis at B3LYP/6-31G method and statistical thermodynamics were obtained and listed in Table 8. It is noted from Table 8 that the standard heat capacities, entropies and enthalpies increase from 10 to 70 K, because the intensities of molecular vibration increase with the increasing temperature. According to the data in Table 8 for the title compound, the corresponding relations between the thermodynamic properties heat capacity, entropies, enthalpies and temperature are described and shown in Fig.6.
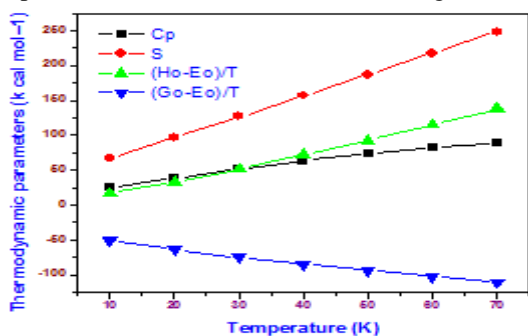
Fig 6. Thermodyna mical parameters of 2-(Trifluoroacetyle)acetophenone.

Table 8. Statistical thermodynamic parameters of 2(trifluoroacetyl)acetophenone at various temperatures.

Temp. (Kelvin)	Thermodynamic parameters (k cal mol⁻¹)			
	C_P	S	$(H^o - E^o_0)/T$	$(G_o - E^o_0)/T$
10	24.499	67.18	16.90	-50.28
20	38.185	97.08	33.04	-64.03
30	51.421	126.75	51.68	-75.07
40	63.645	156.71	71.82	-84.88
50	73.910	187.00	93.04	-93.96
60	82.143	217.56	115.09	-102.47
70	88.707	248.33	137.82	-110.51

9. Conclusion

A complete vibrational analysis of 2(trifluoroacetyle) acetophenone is carried out by HF/6-31G and B3LYP/6-31G basis sets. The influences of fluorine and methyl group to the vibrational frequencies of the title compound were discussed. The observed and stimulated spectra are agreed for the good frequency fit in B3LYP/6-31G basis sets. The difference

between theoretical and experimental wavenumbers within $10cm^{-1}$ is confirmed by the qualitative agreement between the calculated and observed frequencies. Various quantum chemical calculations help us to identify the structural and symmetry properties of the titled molecule. The excellent agreement of the calculated and observed vibrational spectra reveals the advantages of higher basis set for quantum chemical calculations.NBO study reveals that the lone pair orbital participates in electron donation to stabilize the compound. The thermodynamic analysis reveals that the standard heat capacities, entropies and enthalpies increase from 10 to 100 K, because the intensities of molecular vibration increase with the increasing temperature.

References

[1] E. Sittig, R. Marshall, Pharm. Manuf. Encycl. 39 (1988) 177-180.

[2] G. Kumar,B.Tamim, Process Chemistry in the Pharmaceutical Industry, vol. 2, 2007, pp. 142–145.

[3] H.G. Korth, M.I. de Heer, P. Mulder, J. Phys. Chem. 106 (2002) 8779–8789.

[4] P.K. Chowdhry, J. Phys. Chem. A 107 (2003) 5692–5696.

[5] V. Chis, Chem. Phys. 300 (2004) 1–11.

[6] A. Asensio, N. Kobko, J.J. Dannenberg, J. Phys. Chem. A 107 (2003) 6441–6443.

[7] F. Jensen, Introduction to Computational Chemistry, Wiley, New York, 1999.

[8] G. Rauhut, P. Pulay, J. Phys. Chem. 99 (1995) 3093–3100.

[9] P. Sinha, S.E. Boesch, C. Gu, R.A. Wheeler, A.K. Wilson, J. Phys. Chem. A 108 (2004)9213–9217.

[10] M.J. Frisch, G.W. Trucks, H.B. Schlegel, G.E. Scuseria, M.A. Robb, J.R. Cheeseman, J.A. Montgomery, Jr., T. Vreven, K.N. Kudin, J.C. Burant, J.M. Millam, S.S. Iyengar, J. Tomasi, V. Barone, B. Mennucci, M. Cossi, G. Scalmani, N. Rega, G.A. Petersson, H. Nakatsuji, M. Hada, M. Ehara, K. Toyota, R. Fukuda, J. Hasegawa, M. Ishida, T. Nakajima, Y. Honda, O. Kitao, H. Nakai, M. Klene, X. Li, J.E. Knox, H.P. Hratchian, J.B. Cross, C. Adamo, J. Jaramillo, R. Gomperts, R.E. Stratmann, O. Yazyev, A.J. Austin, R. Cammi, C. Pomelli, J.W. Ochterski, P.Y. Ayala, K.Morokuma, G.A. Voth, P. Salvador, J.J. Dannenberg, V.G. Zakrzewski, S.Dapprich, A.D. Daniels, M.C. Strain, O. Farkas, D.K.

Malick, A.D. Rabuck, K.Raghavachari, J.B. Foresman, J.V. Ortiz, Q. Cui, A.G. Baboul, S. Clifford, J.Cioslowski, B.B. Stefanov, G. Liu, A. Liashenko, P. Piskorz, I. Komaromi, R.L.Martin, D.J. Fox, T. Keith, M.A. Al-Laham, C.Y. Peng, A. Nanayakkara, M.Challacombe, P.M.W. Gill, B. Johnson, W. Chen, M.W.Wong, C. Gonzalez, J.A.Pople, Gaussian '03, Revision C. 01, Gaussian, Inc., Wallingford, CT, 2004.

[11] A.D. Becke, J. Chem. Phys. 98 (1993) 5648–5652.

[12] C. Lee, W. Yang, R.G. Parr, Phys. Rev. B 37 (1988) 785–789.

[13] B.D. Becke, Phys. Rev. B 38 (1988) 3098–3100.

[14] J.B. Foresman, A. Frisch, Exploring Chemistry with Electronic StructureMethods, second ed., Gaussian, Inc., Pittsburg, 1996.

[15] S.Y. Lee, B.H. Boo, Bull. Korean Chem. Soc. 17 (1996) 754–759.

[16] P.L. Fast, J. Corchado, H.L. Sanchez, D.G. Truhlar, J. Phys. Chem. A 103 (1999)3139–3143.

[17] M. Kurt, S. Yurdakul, J. Mol. Struct. 654 (2003) 1–9.

[18] T. Sundius, MOLVIB: A program for harmonic force field calculations, QCPE,program No. 807, 20.

[19] V. Krishnakumar, R. John Xavier, Indian J. Pure. Appl. Phys. 41 (2003) 597-600.

[20] S. Chandra, H. Saleem, N. Sundaraganesan, S. Sebastian, Spectrochim. Acta A 74(2009) 704-707.

[21] M.H. Jamroz, J.C. Dobrowolski, R. Brzozowski, J. Mol. Struct. 787 (2006) 172-175.

[22] G. Socrates, Infrared and Raman Characteristic Group Frequencies—Tables andCharts, third ed., Wiley, New York, 2001.

[23] J. Mohan, Organic Spectroscopy—Principles and Applications, Narosa PublishingHouse, New Delhi, 2001.

[24] B. Karthikeyan, Spectrochim. Acta 64 A (2006) 1083-1084.

[25] D. Sajan, I. Hubert Joe, V.S. Jayakumar, J. Raman Spectrosc. 37 (2005) 508–519**.**

[26] P.S. Kalsi, Spectroscopy of Organic Compounds, Wiley Eastern Limited, New Delhi, 1993, pp. 117–118.

[27] A.R. Prabakaran, S. Mohan, Indian J. Phys. 63B (1989) 468–473.

[28] T. Kolev, J. Mol. Struct. 349 (1995) 381–384.

[29] M. Silverstein, G. ClaytonBassler, C. Morrill, Spectrometric Identification of Organic Compounds, Wiley, New York, 1981.

[30] N.B. Colthup, L.H. Daly, S.E. Wiberley, Introduction to Infrared and Raman Spectroscopy, Academic Press, New York, 1964.

[31] V.K. Rastogi, C.B. Arora, S.K. Singhal, D.N. Singh, R.A. Yadav, Spectrochim. Acta53A (1997) 2505–2510.

[32] P.J.A. Ribeiro-Claro, M.P.M. Marques, A.M. Amado, Chem. Phys. Chem. 3(2002)599–606.

[33] A.E. Reed, F. Weinhold, J. Chem. Phys. 83 (1985) 1736–1740.

[34] A.E. Reed, R.B. Weinstock, F. Weinhold, J. Chem. Phys. 83 (1985) 735–746.

[35] A.E. Reed, F. Weinhold, J. Chem. Phys. 78 (1983) 4066–4073.

[36] J.P. Foster, F. Weinhold, J. Am. Chem. Soc. 102 (1980) 7211–7218.